electronics

MDPI

Article

Bi-Level Optimization Model for DERs Dispatch Based on an Improved Harmony Searching Algorithm in a Smart Grid

Hongsheng Su [1,2,*], Xingsheng Wang [1] and Zonghao Ding [1]

[1] School of Automation and Electrical Engineering, Lanzhou Jiaotong University, Lanzhou 730070, China; 12221544@stu.lzjtu.edu.cn (X.W.); 12221504@stu.lzjtu.edu.cn (Z.D.)
[2] Rail Transit Electrical Automation Engineering Laboratory of Gansu Province, Lanzhou Jiaotong University, Lanzhou 730070, China
* Correspondence: suhs@mail.lzjtu.cn

Abstract: To satisfy the large-scale grid-connected demands of distributed energy resources (DERs), a bi-level optimization model is proposed for private DER dispatch managed by a virtual power plant (VPP) in a smart grid environment in this paper. The optimization models of the upper and lower layers serve as the planning layer and the operational layer, respectively, wherein the upper optimization model is mainly aimed at the optimization allocation of DERs under an unchanged network topology, and the lower-level optimization model is mainly responsible for the optimization of the distributed network topology from the optimization results of the upper layer. An improved harmony searching algorithm (HSA) is then applied to resolve the model through continuous iterations and communications between the upper and lower levels until an expected aim is achieved, which can satisfy the aim demand of the upper and the lower levels at the same time. Finally, six optimization scenarios are planned and selected in order to evaluate the performance of the bi-level optimization strategy in the IEEE33 bus distribution system and the 69-bus distribution system, and the optimized results show that the proposed method can effectively improve the grid-connected capacity of DERs and their system performance, and are more flexible in facing a growing ambient smart environment.

Keywords: distributed energy resources (DERs); dispatch; distribution network; bi-level optimization; harmony search algorithm (HSA); smart environment

check for updates

Citation: Su, H.; Wang, X.; Ding, Z. Bi-Level Optimization Model for DERs Dispatch Based on an Improved Harmony Searching Algorithm in a Smart Grid. *Electronics* **2023**, *12*, 4515. https://doi.org/10.3390/electronics12214515

Academic Editor: Ahmed Abu-Siada

Received: 3 October 2023
Revised: 23 October 2023
Accepted: 25 October 2023
Published: 2 November 2023

Copyright: © 2023 by the authors. Licensee MDPI, Basel, Switzerland. This article is an open access article distributed under the terms and conditions of the Creative Commons Attribution (CC BY) license (https://creativecommons.org/licenses/by/4.0/).

1. Introduction

With the gradual shortage of traditional fossil fuels and worsening environmental issues, the exploration and utilization of renewable energy are becoming increasingly more significant. Distributed energy resources (DERs), represented by wind energy, photovoltaic (PV), controllable loads, and electric cars, can effectively alleviate the energy shortage and provide green power to users in such a way that it has become an important development direction in which to realize energy saving and emission reduction for electric power systems [1]. As a clear energy, DERs are thought to possess the advantages of low pollution emission, flexibility convenience, high reliability, etc., such that they can strengthen the capabilities of distributed networks to resist natural disasters and other risks [2]. Hence, DERs are advocated and grid connected in order to speed up the development of various forms of renewable energies. However, at the same time, due to the stronger characteristics of DERs, such as randomness, intermittence, smaller capacity, large quantity, and uneven distribution, the complexities and uncertainties of the system increase, such as the power flow direction, network loss, line blocking, voltage flicker, harmonic effect, etc., which make system management difficult and block the large-scale grid connection of DERs. In China, a micro-grid is often adopted for grid-connected DERs, which can effectively coordinate the technical contradiction between the large power grid and diverse distributed generations (DGs), and possesses certain energy management functions. However, a micro-grid often

requires the local application of DGs and its users as its main control goal, being restricted by geographical area, which makes the utilization of multi-area large-scale DGs and their scale benefits in the power market limited. Active distribution networks are another effective solution by which to achieve large-scale grid-connected operations of DGs, which can extend the access radius of DERs to a certain extent, but the benefits that DGs offer to a large power grid and the electricity market are not considered enough. However, the presentation of a virtual power plant (VPP) provides new ways by which to solve the issue [3]. Just as virtual utilities make use of emerging technologies to provide consumer-oriented electricity services, a VPP does not change the grid-connected pattern of each DG, but aggregates all types of DERs into an integrated entity to realize fully coordinated optimization through advanced control, measurement, communication, and other technologies. Clearly, this is more conducive to the rational allocation and utilization of DER resources. A VPP emphasizes the functions and effects presented, which helps to modernize the concept of operation and produces social and economic benefits, and the basic application scenario of which is applicable to the electricity market. Simultaneously, the VPP, together with DERs visualization, can greatly reduce the impact of grid-connected DG and the scheduling difficulty brought about by DG growth, which makes the distribution management more flexible and orderly, and the stability of the system's operation is also ensured [4]. On the other hand, with the help of advanced computers, communication, automation control, and wide-area measurement technologies, a distributed grid can flexibly change its construction to suit the grid-connected DERs managed by VPPs, such that the largest benefits possible will be achieved. Thus, we can determine that the distributed grid possesses intelligence, called a smart grid, and DERs (DGs) managed by VPPs also demonstrate human-like behaviors. Of course, the key to realizing this technology lies in the dispatch algorithm between the smart grid and VPPs.

1.1. Literature Review

For a conventional distributed network, to meet the larger-scale access requirements of DGs, researchers have already conducted a number of studies and accumulated valued experience. Yu and Zhang proposed an improved immune genetic algorithm (IMA) to solve the problem of a distributed network structure with minimum grid loss as the aim, wherein a probability selection method was proposed with a vectorial moment based on ensuring the diversity of the solution space in [5]. An improved node-stratified forward-backward sweep flow calculation was proposed to improve the adaptability of the power flow algorithm pertaining to the change in network topology based on graph theory in [6]. The randomness of wind power output was considered and the randomness of the DGs was also approximately treated using the scene partitioning method with probability in [7], which effectively solved the influence of wind power random outputs on the distribution network topology. However, the above studies only started with a single-aim function to optimize the distribution network structure with minimum active power loss, and did not consider multi-objective optimization, which led to serious defects in the comprehensive indexes of the optimized systems. In [8], a genetic algorithm (GA) with self-adaptively adjusted crossover and a mutation operator was applied to improve the performance of the algorithm in the dynamic reconfiguration of the distribution network, but there still existed some defects with longer iteration times. The outputs of DGs, together with their switching states, were selected as objective functions, and the leapfrog algorithm was then applied to optimize the distribution network structure in [9]. To a certain extent, the algorithm easily solved the problem of trapping the local optimum, but it produced a large number of infeasible solutions. In [10], Chen and Zhang proposed a self-adaptive multi-objective particle swarm optimization algorithm based on Pareto. It could effectively expand the search space and ensure the diversity of the solution vectors, but there were some defects with larger calculation quantities. The above three investigations only considered the distribution network configuration in terms of the algorithms and lacked a study of the optimized issue itself. To avoid the generation of infeasible solutions, some scholars have

started with the distribution network topology to search for effective simplified methods. According to the characteristics of a distributed network, an effective coding method was applied to allow the switches not in the loop to be normally open and not participate in the process of optimization; thus, the distributed network topology was effectively simplified in [11]. In [12], the divide-and-conquer method was applied based on the parallel tabu search algorithm to expand the search space by providing diverse tabu lists for diverse subspaces in the solution space. In [13], an optimization method combining loop group searching and dividing ring substitution strategies together was proposed, which could effectively reduce the search space and improve the efficiency of optimization. In [14], a new bi-level optimization method was proposed based on the power moment and neighborhood search, which could reduce the calculation amount and improve the feasibility of the solutions. However, the above methods are only applicable to a simple network structure, and cannot be used to solve the problem of infeasible solutions for complex multi-ring networks. In addition, they do not consider the impact of the acceptable capacities of DGs on the distribution network topology. To address these issues, Nasiraghdam and Jadid regarded the distribution network topology and power configuration of DGs as a nonlinear optimization aim, and applied the artificial bee colony (ABC) algorithm to optimize the distribution network structure in [15]. In [16], a stepwise heuristic algorithm and sensitivity index were adopted to realize the joint optimization of the distribution network structure and DGs allocation. Although the above investigations consider the effect of DG output on the distribution network structure, the installation sites of the DGs are still not included in the optimization process, which leads to certain limitations. In other studies, the optimization configuration of DGs only acted as a simple initial condition in the process of distribution network configuration [17,18]. However, the impact of the interaction between the acceptable capacity of DGs and the distribution network topology has not been better reflected. In [19], the authors modeled Internet data center energy consumers based on Internet services, but did not consider DG access. In [20], the development of an optimal scheduling model that takes into account the charging behavior of electric vehicles and consumer economics was presented; however, it does not take into account the network topology of the distribution network. Mansouri, S.A. et al. proposed a new framework for micro-grid scheduling and distribution feeder reconfiguration in [21]; however, there were no DG locations and capacities included. In [22], the authors investigated the problem of the distributed cooperative energy management of multiple energies; however, no description of the distribution network topology was carried out.

1.2. Methodology and Organization of the Article

In view of the aforementioned shortcomings in existing DG access methods in distributed networks, which are static less than ideal, especially under VPP and smart grid scenarios, this paper proposes a dual-layer optimization model for both distributed network topology and DER configuration. In this model, the upper optimization model is mainly aimed at improving the grid-connected capacities of the DGs, while the lower-level optimization model mainly counters the optimization of distribution network topology. During the iteration process, the upper and lower level optimization models communicate and influence each other, such that the optimization process possesses stronger relevance, i.e., this means that the optimization results of the upper and lower layer are transmitted and transferred to each other in each iteration, until the desired result is ultimately achieved. Thus, it can determine the optimal network structure and the best acceptable capacities of the DGs, and better balance the optimizing aims of the upper and lower, such that the established system possesses certain stability and safety. To solve the bi-level operation model, we propose an improved harmony searching algorithm (HSA) to accelerate convergence. The proposed optimized model takes into reliability and economy, ensuring the safe and cost-effective operation of the distribution network; additionally, the grid-connected capacities of the DGs are significantly improved, and the compatibility between the DGs

and distributed network is greatly enhanced and especially suitable under a smart grid environment.

2. Bi-Level Optimization Model

2.1. Upper-Level Aim Function

The fixed position and capacity of DERs or DGs can lead to problems such as the DGs being unable to match the loads and excessive construction of DGs, which will affect the acceptable capacities of DGs. Therefore, the upper optimization model is used as the planning layer of the bi-level optimization model, primarily responsible for determining the location and capacity of each DG. Its main purpose is to eliminate the disadvantage of the optimization model for distribution network topology, which is used to improve the acceptable capacities of the DGs but cannot ensure that DGs can access the distribution network with maximum permitted capacity.

2.1.1. Determination of DG Position

DGs accessed distribution network will generate a non-negligible impact on the node voltage of the system, such that each node-voltage level will change with the difference of DG location accessed. In order to optimize the configuration of DGs and improve the system voltage level, the locations and capacities of the grid-connected DGs should be rationally balanced. The voltage stability index (VSI) is an indicator that reflects the voltage stability of electric power systems, its magnitude can indicate whether the bus voltages are good or bad. Therefore, VSI is used to determine the installation locations of the DGs in the distribution network in this paper. Assume that there is a branch k as shown in Figure 1, the VSI of which can be described by [23]

$$VSI_{(i+1)} = \left|V_i\right|_4 - 4(P_{Li+1}X_k - Q_{Li+1}R_k)^2 - 4(P_{Li+1}R_k + Q_{Li+1}X_k)\left|V_i\right|_2, \quad (1)$$

where P_{Li+1} and Q_{Li+1} are active power and reactive power flowing into the $(i+1)^{th}$ node, respectively, R_k and X_k are the resistance and reactance of the branch k, and V_i expresses the voltage of the node i.

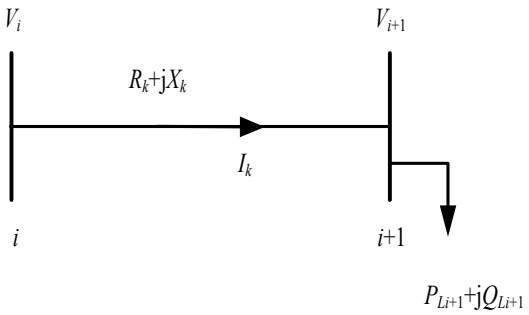


Figure 1. Typical branch of simple distribution network.

Based on the relevant knowledge of VSI, the locations of the DGs accessing the distribution network can be determined by using the maximum variation of VSI as the objective function by

$$f_1 = \Delta VSI = max\left(\frac{1 - VSI_i}{1}\right) i = 2, 3, \ldots, N_{bus} \quad (2)$$

The VSI_i in (2) can be obtained through power flow calculations arranged in ascending order, which can be used to rank the order of the nodes for DG configuration. If a node has a higher VSI, the stability of the related node is better, so there is no necessary access DGs. On the contrary, the stability of the node is worse, such that it is necessary to improve the bus voltage stability by accessing DG.

Each node voltage should satisfy the following constraints.

$$V_i^{min} \le V_i \le V_i^{max} \quad i = 1, 2, \cdots, N_{bus}, \tag{3}$$

where V_i^{max} and V_i^{min}, respectively, are the upper and lower limits of the node i.

2.1.2. Determination of DG Capacity

As DGs access distribution network, the power flow direction in the system may change. The branch loss of the system can be reduced by reasonably DGs accessed, however, excessive DG capacities can have adverse effects, such as the reverse power flow, which will lead to an increase in branch network loss. Hence, the sizes of the DGs accessed to the distribution network possess larger impacts on system grid loss so as not to be able to be ignored [24]. Therefore, in this paper, the grid-loss reduction amount is used as the objective function to determine the capacity of each DG connected to the distribution grid. As shown in Figure 2, let us assume that there is a branch k with its first node i and the last one $i + 1$: if a DG is connected to any location in the distribution network, the power loss after DG is connected can be expressed as [25].

$$P_{\text{Loss}} = \frac{R_k}{V_i^2}\left(P_k^2 + Q_k^2\right) \tag{4}$$

$$P_{\text{Loss}}^{\text{DG}} = \frac{R_k}{V_i^2}\left(P_k^2 + Q_k^2\right) + \frac{R_k}{V_i^2}\left(P_{\text{DG}}^2 + Q_{\text{DG}}^2 - 2P_kP_{\text{DG}} - 2Q_kQ_{\text{DG}}\right)\left(\frac{G}{L}\right) \tag{5}$$

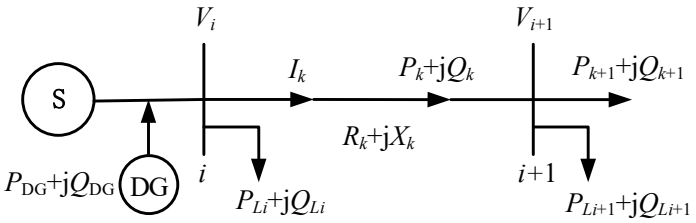


Figure 2. Distribution system with DG installation.

Hence, the grid-loss reduction amount before and after the DG accessed can be expressed by

$$\Delta P_{\text{Loss}}^{\text{DG}} = \frac{R_k}{V_i^2}\left(P_{\text{DG}}^2 + Q_{\text{DG}}^2 - 2P_kP_{\text{DG}} - 2Q_kQ_{\text{DG}}\right)\left(\frac{G}{L}\right), \tag{6}$$

where $\Delta P_{\text{Loss}}^{\text{DG}}$ is the power loss when DG is accessed to the distribution network, P_k and Q_k are the real power and reactive power flowing from node i, P_{DG} and Q_{DG} are the real power and reactive power supplied by DGs, R_k is the resistance of branch k, V_i is the voltage of the node i, G is the distance from source to DG location, L is the distance from source to the load node.

According to the above analysis, if $\Delta P_{\text{Loss}}^{\text{DG}}$ is positive, the system grid loss will lessen after DGs accessed, and will increase otherwise. Therefore, the maximum reduction amount of grid loss before and after the DG accessed is used as the objective function to determine the capacity of the DG connected to the distribution grid, which can be described by

$$f_2 = \max\left(\Delta P_{\text{Loss}}^{\text{DG}}\right) \tag{7}$$

In summary, the objective function of the upper optimization model consists of Formulas (2) and (7), which determine the acceptable capacity of the DG. The upper layer optimization model considers the impact of the acceptable capacity of the DG on the distribution network, effectively avoiding the disadvantage that the active power loss caused by the maximum consumption of DG as the goal is not the optimal one. Additionally, it provides a reasonable basis for the optimization of the lower-layer model.

The constraint conditions of the DGs accessed to the network are

$$\begin{cases} 0 \le P_{\mathrm{DG},n} \le P_{\mathrm{DG},n}^{\max} & n = 1, 2, \cdots, N_{\mathrm{DG}}; \\ 0 \le Q_{\mathrm{DG},n} \le Q_{\mathrm{DG},n}^{\max} & n = 1, 2, \cdots, N_{\mathrm{DG}}; \end{cases}, \tag{8}$$

where $P_{\mathrm{DG}}^{\max}$ and $Q_{\mathrm{DG}}^{\max}$ are the maximum active and reactive power of the DG accessed to the distribution network.

2.2. Lower-Level Aim Function

The lower-level optimization model serves as the operational layer of the bi-level optimization model. It optimizes distribution network topology based on the acceptable capacities of the DGs provided by the planning layer. It then determines the optimal topology of the distribution network and returns it to the planning layer as part of the optimization objective function. Based on the relevant knowledge of distribution network reconfiguration modeling, the establishment of the objective function is primarily the aspects of economy and reliability. This includes reducing network loss, balancing load, and improving voltage distribution. Therefore, the network loss together with the load balance degree is considered to select as the optimized aim of the lower level for distribution network reconfiguration. Assume that there is a branch k with the starting node i and the end node $i + 1$ as shown in Figure 3, and the grid loss of the branch can be expressed by

$$P_{\mathrm{Loss}}(i, i+1) = R_k \frac{(P_k^2 + Q_k^2)}{|V_i|^2} \tag{9}$$

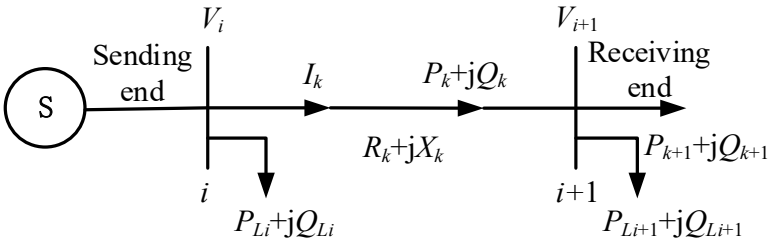


Figure 3. Before and after reconfiguration of distribution system.

Hence, the total grid loss before reconfiguration can be written by

$$P_{\mathrm{T,Loss}} = \sum_{i=1}^{n} P_{\mathrm{Loss}}(i, i+1), \tag{10}$$

where P_{Loss} is network loss of the branch k, and $P_{\mathrm{T,Loss}}$ is total network loss before reconfiguration, P_k and Q_k are real power and reactive power flowing out of the node i, R_k is resistance of the branch k, and V_i is the voltage of the node i.

Likewise, the network loss of the branch k after reconfiguration can be given by

$$P'_{\mathrm{Loss}}(i, i+1) = R_k \frac{(P_k'^2 + Q_k'^2)}{|V_i'|^2} \tag{11}$$

Thus, the loss after reconfiguration is written by

$$P'_{\mathrm{T,Loss}} = \sum_{i=1}^{n} P'_{\mathrm{Loss}}(i, i+1), \tag{12}$$

where P'_{Loss} is power loss of the branch k after reconfiguration, $P'_{\mathrm{T,Loss}}$ is gross power loss after reconfiguration, P'_k and Q'_k are real power and reactive power flowing out of the node

i after reconfiguration, R_k is resistance of the branch k, and V' is the voltage of the node i after reconstruction.

The gross loss reduction amount before and after reconfiguration can be expressed by

$$\Delta P_{\text{Loss}}^{\text{R}} = \sum_{i=1}^{n} P_{\text{T,Loss}}(i, i+1) - \sum_{i=1}^{n} P'_{\text{T,Loss}}(i, i+1), \tag{13}$$

where $\Delta P_{\text{Loss}}^{\text{R}}$ is the gross loss reduction amount before and after reconfiguration.

In terms of economy, the objective function is formulated to make the amount of network loss reduction maximum. After standardization, the aim function can be written by

$$f_3 = \max\left(\frac{\Delta P_{\text{Loss}}^{\text{R}}}{P_{\text{T,Loss}}}\right) \tag{14}$$

On the other hand, for reliability, the objective function can be formulated to let the variation of load balance maximum, which can be described by [26].

$$f_4 = \max\left[\left|1 - \sum_{k=1}^{N_b}\left(\frac{S_k}{S_k^{\max}}\right)^2\right|\right] = \max\left[\left|1 - \sum_{k=1}^{N_b}\frac{P_k^2 + Q_k^2}{\left(S_k^{\max}\right)^2}\right|\right], \tag{15}$$

where S_k and $S_k^{\max}$, respectively, express complex power and maximum complex power injecting into branches k, P_k, and Q_k are active power and reactive power of sending end, and N_b is the branches number of the systems.

The load balance does not have a simple positive correlation with network loss. This means that network loss is not optimal when load balance is optimal, and vice versa. Hence, the lower-level objective function selects both grid loss and load balance degree as optimizing aims, which can be given by

$$F = w_1 f_3 + w_2 f_4 \tag{16}$$

In addition, the following constraints must be satisfied during reconfiguration.

2.2.1. Power Flow Constraint

$$\begin{cases} P_i - V_i \sum\limits_{j=1}^{N_{bus}} Y_{ij} V_j \cos\left(\delta_i - \delta_j - \theta_{ij}\right) = 0 \quad i = 1, 2, \cdots, N_{bus} \\ Q_i - V_i \sum\limits_{j=1}^{N_{bus}} Y_{ij} V_j \sin\left(\delta_i - \delta_j - \theta_{ij}\right) = 0 \quad i = 1, 2, \cdots, N_{bus} \end{cases}, \tag{17}$$

where P_i and Q_i are active and reactive power injecting into the node i, V_i and V_j are the voltages of node i and node j, Y_{ij} is admittance between the node i and the node j, δ_i and δ_j are voltage phase angle of the node i and j, and θ_{ij} is admittance angle between the node i and j.

2.2.2. Node Voltage Constraint

$$V_i^{\min} \le V_i \le V_i^{\max} i = 1, 2, \cdots, N_{bus}, \tag{18}$$

where $V_i^{\min}$ is the lower voltage limit of the node i, and V_i is the voltage of the node i, and $V_i^{\max}$ is the upper voltage limit of the node i.

2.2.3. Branch Current Constrain

$$0 \le I_k \le I_k^{\max} k = 1, 2, \cdots, N_b, \tag{19}$$

where I_k is the current flowing through the branch k, and $I_k^{\max}$ is maximum permissible current of the branch k.

2.2.4. Network Topology Constraint

The network topology remains unchanged before and after distribution network reconfiguration; that is, $g_k \in$ G, wherein g_k represents the network topology reconfigured, and G is a set of all feasible radiant shape networks.

3. Coding Principle of Reconfiguration Ring

The distribution network consists of two types of switches: a large number of section switches and a small number of tie switches. The operation mode of these switches is described as a closed-loop design and open-loop operation. Based on the operation mode, it is known that the distribution network can form a basic loop by closing a tie switch. Additionally, the network can be maintained by disconnecting any section switches within the loop. Hence, it is necessary to select reasonable coding methods in order to effectively reduce the search space and improve the efficiency of problem-solving optimization.

3.1. Basic Ring Matrix

The basic ring in a distribution network is defined as a loop formed by one tie switch and several section switches. The number of tie switches in the basic ring corresponds to the number of basic rings in a distributed network. Taking the IEEE33 bus distribution system as an example in Figure 4, the system consists of 32 section switches and 5 tie switches, so it contains 5 basic rings.

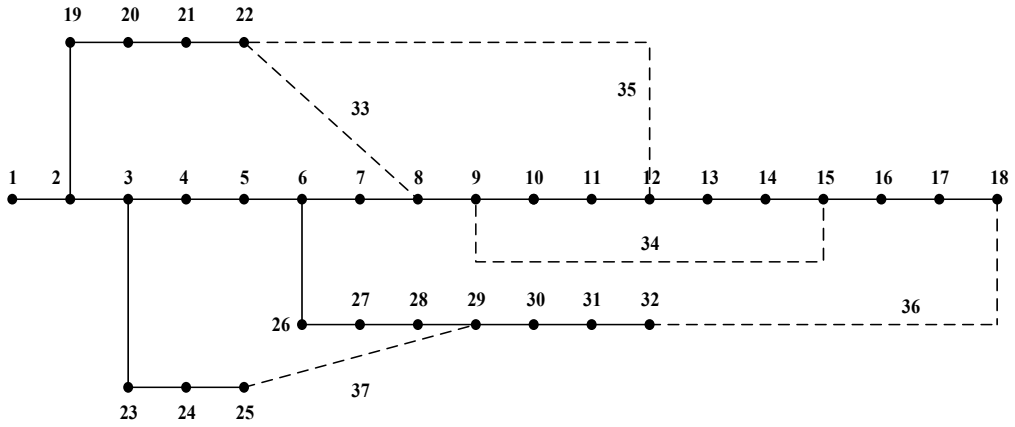


Figure 4. IEEE 33-node distribution system.

The basic ring matrix can be described by $M = (M_{ij})$, i = 1,2, . . ., n, and j = 1,2, . . ., m, wherein i stands for the number of the basic ring, and j represents the position of the section switches in the branch of the basic ring. If the number of section switches in a basic ring is less than the maximum value, the remaining elements are filled with 0. It is worth noting that in most studies, the switches in a distribution network are not represented in the form of a basic ring matrix. In this paper, the basic ring matrix is generated according to [27]. The basic ring matrix of the IEEE 33 bus distribution system is described by

$$M = \begin{bmatrix} 7 & 6 & 5 & 4 & 3 & 2 & 20 & 19 & 18 & 0 & 0 & 0 & 0 & 0 & 0 & 0 & 0 & 0 & 0 & 0 & 0 \\ 14 & 13 & 12 & 11 & 10 & 9 & 0 & 0 & 0 & 0 & 0 & 0 & 0 & 0 & 0 & 0 & 0 & 0 & 0 & 0 & 0 \\ 11 & 10 & 9 & 8 & 7 & 6 & 5 & 4 & 3 & 2 & 21 & 20 & 19 & 18 & 0 & 0 & 0 & 0 & 0 & 0 & 0 \\ 17 & 16 & 15 & 14 & 13 & 12 & 11 & 10 & 9 & 8 & 7 & 6 & 32 & 31 & 30 & 29 & 28 & 27 & 26 & 25 & 0 \\ 24 & 23 & 22 & 28 & 27 & 26 & 25 & 5 & 4 & 3 & 0 & 0 & 0 & 0 & 0 & 0 & 0 & 0 & 0 & 0 & 0 \end{bmatrix}$$

3.2. Topology Simplification of Distribution Network

As the distribution network is reconfigured, the number of tie switches is equal to the number of solutions, and the dimension of each solution vector is the same as the total number of basic ring switches [25]. The traditional encoding method uses a binary encoding rule, where a value of 1 represents a closed switch and a value of 0 represents an open switch. With the increasing complexity of the distribution network topology, the number of solution vectors will also increase, such that the search space will increase sharply with geometric progression. Taking the IEEE 33 bus distribution system as an example, there are a total of 37 switches, 32 section switches, and 5 tie switches, so there are 2^{37} states that exist in the search space. However, despite the multitude of switch states, many of them are infeasible solutions involved in these switch states, which will seriously affect the speed and quality of search optimization. Hence, it is crucial to simplify the distribution network topology in order to address this issue.

This paper aims to simplify the distribution network topology by utilizing the relevant knowledge of graph theory. Let us use $G = (V, E)$ to express a graph, wherein V expresses nodes and E represents edges, x is an arbitrary node in G, and the number of edges associated with node x is denoted as the degree of x and expressed by $d(x)$. Among them, the number of edges injected into the node x is called indegree of x, and is represented by $d^+(x)$. The number of edges flowing out the node x is called outdegree of x, and expressed by $d^-(x)$.

Based on the related knowledge of graph theory and the structural characteristics of the distribution network, the principle of topological simplification can be summarized as follows.

- The branches directly connected to the power source node cannot be coded;
- For an independent branch that does not form a loop, if the switch related to it is disconnected, an isolated island will be formed, and so it cannot be coded;
- Based on the knowledge related to node degree, close all the switches in the network. Merge the branches between nodes where the sum of their indegrees and outdegrees is less than or equal to 2 into one branch, which is denoted as a branch group.

3.3. Modification of Infeasible Solution

For infeasible solutions, there are two main ways applied to modify them. The first approach is to reduce the probability of generating solution vectors that do not satisfy the constraints by implementing effective coding rules. The second approach is to apply relevant strategies to enhance the efficiency of generating feasible solutions that meet the constraint conditions. In this paper, the first strategy is adopted to modify the infeasible solutions, and the specific schemes are as follows.

- Only one branch can be disconnected for each basic ring, otherwise, an isolated island will be formed;
- If multiple basic rings have included relationships, the basic ring with more section switches will be disconnected first. Then, the rings will be broken up in order of their size, with only one branch being disconnected in the public branch group, at most;
- If there are pairwise intersecting relationships between multiple basic rings, with each ring having at least their basic rings, then there will be at least one closed branch in the public branch group;
- If multiple basic rings simultaneously meet the above two conditions, and there is a public branch disconnected between one basic ring and the remaining N-1 basic rings, without including public branch sets of N basic rings, then it may be acceptable for the disconnected branches to exist in the public branches of N basic rings.

4. Discussion

4.1. Improved Harmony Search Algorithm

Inspired by the process of musicians repeatedly adjusting the pitch of their instruments and ultimately achieving a wonderful harmony, Geem et al. [28] proposed a new heuristic

searching algorithm denoted as the harmony search algorithm (HSA). This algorithm possesses characteristics such as a simple structure, few parameters, and easy implementation, making it widely applicable to various scenarios of global optimization [29,30]. The process of the algorithm is described as follows.

1. Firstly, the HSA includes five parameters: harmony memory (HM), harmony memory size (HMS), harmony memory considering rate (HMCR), pitch adjusting rate (PAR), and bandwidth (bw);
2. To initialize the harmony memory, the matrix from HM can be expressed as shown in (20), wherein x represents the randomly generated solution vector;

$$HM = \begin{bmatrix} x_1^1 & x_2^1 & \cdots & x_{N-1}^1 & x_N^1 \\ x_1^2 & x_2^2 & \cdots & x_{N-1}^2 & x_N^2 \\ \vdots & \vdots & \vdots & \vdots & \vdots \\ x_1^{HMS} & x_2^{HMS} & \cdots & x_{N-1}^{HMS} & x_N^{HMS} \end{bmatrix} \tag{20}$$

3. Improvise a new harmony: There are three main parameters involved in a new generation of harmony vectors, i.e., HMCR, PAR, and bw. Assuming that the new harmony is $x' = \begin{bmatrix} x_1' & x_2' & \cdots & x_N' \end{bmatrix}$, and it is then generated below:
   - Firstly, to generate a random number rand1 in the range of 0 to 1 following uniformly distributed. If rand1 < HMCR, then the new solution is selected from HM with the rate of HMCR, and denoted by $x_i' \leftarrow x_i' \in \left\{x_i^1, x_i^2, \cdots, x_i^{HMS}\right\}$. Otherwise, it is randomly selected from the outside of HM with the rate of (1-HMCR), and denoted by $x_i' \leftarrow x_i' \in X_i$;
   - If the new solution x_i' is selected from HM, that is, $x_i' \leftarrow x_i' \in \left\{x_i^1, x_i^2, \cdots, x_i^{HMS}\right\}$, then it randomly generates a number rand2 in the range of 0 to 1 following a uniform. If rand $2 < PAR$, the new solution will be generated according to $x_i' = x_i' \pm rand2 \times bw$. Otherwise, it will keep unchanged, that is, $x_i' = x_i'$.
4. Repeat the above steps until a completely new harmony vector is generated;
5. Update the harmony memory by comparing the fitness value of the new harmony vector with the worst harmony vector in the HM, and if the fitness value of the new harmony vector is better, it replaces the worst harmony vector; otherwise, the newly generated harmony vector is removed from the HM;
6. Check the termination conditions. If the maximum number of iterations has not been reached, repeat steps 3 and 4; otherwise, terminate the process.

In most of the literature, the parameters of HSA are fixed in advance, which can lead to the algorithm getting stuck in local optimization [31]. Therefore, it is recommended to dynamically adjust the relevant parameters during the iteration process to expedite convergence. The proposed method for improvement is as follows.

1. Improvement of parameters: Based on the search mechanism of HSA, during the early stage of optimization, it is recommended to select solution vectors in HM with a larger HMCR and a small PAR, considering the larger search space, whereas in the later period, with the solution vectors updated and the optimized space condensed, the new solution vector in HM need to be selected with smaller HMCR and larger PAR to prevent falling into local optimization. The parameters improvement can be written by

$$\begin{cases} HMCR_i = HMCR_{\max} - \alpha(HMCR_{\max} - HMCR_{\min}) \\ PAR_i = PAR_{\min} + \alpha(PAR_{\max} - PAR_{\min}) \end{cases}, \tag{21}$$

$$\alpha = \frac{F_{\max} - F_{avg}}{F_{\max} - F_{\min}}, \tag{22}$$

where $F_{\max}$ is maximum fitness in HM, $F_{\min}$ is minimum fitness in HM, F_{avg} is the average fitness in the whole HM.

2. Judgment of local optimization. To enhance the accuracy of the optimization process, more accurate, a local optimal judgment mechanism is added by

$$\sigma^2 = \frac{1}{HMS}\sum_{i=1}^{HMS}(F_i - F_{avg})^2, \tag{23}$$

where σ^2 is the fitness variance of the solution vectors, F_i is the fitness of ith harmony, and F_{avg} is the average of fitness in the whole HM.

σ^2 can reflect the degree of deviation between the fitness value of a specific harmony and the expected fitness value. The larger it is, the more the deviation degree is, which means it is easier to fall into the local optimization. On the contrary, it is more reasonable for the optimization process.

4.2. Model Optimization Based on Improving HSA

To address the issues of improving the acceptable capacity of DG that is not included in most existing distribution network reconfigurations involving DG, this paper proposes a double-layer nested loop solution to optimize the distribution network reconfiguration. The upper optimization model focuses on enhancing the acceptable capacity of DG and serves as the planning layer responsible for making optimal decisions regarding the acceptable capacity of DG. The lower layer optimization model primarily focuses on optimizing the distribution network reconfiguration and serves as the operational layer responsible for making optimal decisions regarding network topology. The dual-layer optimization model is interactive, with the running layer utilizing the decision results transmitted by the planning layer to optimize the topology. Simultaneously, the optimization of the acceptable capacity of DG in the planning layer is based on the upward feedback from the decision making in the running layer.

The bi-level optimization model proposed in this paper is a multi-constrained and multi-objective optimization problem. It is optimized using the improved HSA, which includes the optimization of both the network topology and the acceptable capacity of DG. As explained in Section 3.2, the essence of distribution network reconfiguration lies in the exchange of switching states between the normally opened tie switches and the normally closed section switches. Hence, the optimized solution vectors consist of two parts. The first part includes the switching states, while the second part comprises the locations and capacities of the DGs. In a study by Mistry and Roy [32], the relationship between the number of DGs connected to the distribution network and network loss was analyzed. It was found that the rate of network loss reduction does not show a significant improvement or may even decrease when the number of DGs connected to the system exceeds three. Therefore, in this paper, a total of three DGs are selected to be connected to the distributed network. Known from the above analysis, a solution vector can be constructed by

$$HM^i = \begin{bmatrix} T_1^i & T_2^i & T_3^i & \cdots & T_m^i & S_{n1}^i & S_{n2}^i & S_{n3}^i \end{bmatrix}; \tag{24}$$

where T_m^i represents the position of the disconnected switch in the basic loop group with the *i-th* solution vector and the *m-th* is basic loop group, and S_n^i is the capacity of the DG with the *i-th* DG in the *n-th* node.

All the solution vectors of the bi-level optimization model can be generated in accordance with HM^i, and must satisfy the constraint conditions of the upper and lower-layer optimization models. Additionally, they should also satisfy the radial operating conditions of the distributed network. The solution vectors of the entire optimization model are given by

$$HM = \begin{bmatrix} T_1^1 & T_2^1 & \cdots & T_m^1 & S_{n1}^1 & S_{n2}^1 & S_{n3}^1 \\ T_1^2 & T_2^2 & \cdots & T_m^2 & S_{n1}^2 & S_{n2}^2 & S_{n3}^2 \\ \vdots & \vdots & \vdots & \vdots & \vdots & \vdots & \vdots \\ T_1^N & T_2^N & \cdots & T_m^N & S_{n1}^N & S_{n2}^N & S_{n3}^N \end{bmatrix} \tag{25}$$

The concrete solving steps can be described in detail as follows.

1. Input the original data, preprocess them, and set up the parameters of the improved HAS;
2. Determine the installation position and capacity of DGs according to the VSI and $\Delta P_{\text{Loss}}^{\text{DG}}$ in the upper optimization model. These values are used as the solution vector of the upper-level optimization model, save them and the topology of the distribution network in HM;
3. Use the solution vector generated in step 2 as the initial value in the lower optimization model. Then, apply the improved HSA to perform the lower-level optimization, which will determine the new distribution network structure. Finally, update the HM with the new information;
4. To determine the termination conditions, check if they are satisfied. If the conditions are met, the iteration stops and proceeds to step 5. Otherwise, return to step 2;
5. Output the optimized solution vectors.

5. Examples

To verify the effectiveness of the bi-level optimal model proposed, we select the IEEE 33-bus system and 69-bus system for application in this paper. The optimization procedure utilized the improved HSA mentioned in Section 4, with specific parameters set by $HMS = 50$, $HMCR_{max} = 0.95$, $HMCR_{min} = 0.65$, $PAR_{max} = 0.7$, $PAR_{min} = 0.1$, $w_1 = 0.5$, $w_2 = 0.5$, and $Itr_{max} = 300$, wherein Itr_{max} is the maximum iteration times.

A dual-layer optimization model is presented in this paper from the mutual connections between distributed grid reconfiguration and the DG allocation so as to win an economic and reliable operation for the distributed grid. To validate this approach, the optimization model is divided into six scenarios, as shown in Table 1. Among these scenarios, scenario 6 is particularly suitable for VPP and smart grid. In addition, in order to comprehensively represent the load situations, the load levels are categorized into three types using load level coefficients, that is, light, nominal, and heavy, respectively, 0.5, 1.0, and 1.6. According to Section 4.2, three DGs are designed to be integrated into the system.

Table 1. Scenario division of the system.

Scenario	Specific Division
Scenario 1	Original state without DGs and reconfiguration
Scenario 2	Only reconfiguration
Scenario 3	Only DG allocation
Scenario 4	DG allocation after reconfiguration
Scenario 5	Reconfiguration after DG allocation
Scenario 6	Dual-layer optimization

5.1. 33-Bus Test System

The 33-node system consists of 37 branches, with a system voltage of 12.66 kV and a total load of 3715 kW + j2300kvar, and the system parameters and load data refer to [33].

The system is optimized under six scenarios and three different load levels using the proposed improved optimization model. The optimized results are presented in Table A2 of Appendix A. Taking the scenarios with a load level coefficient of 1.0 as examples, we observe that in the original state, where no optimization measures are taken, the system experiences a grid loss of 202.6471 kW and a minimum voltage magnitude of Vmin = 0.9133 p.u at node 18. These results are consistent with those reported in [21,30], as shown in Table A2 of Appendix A. This confirms the correctness and effectiveness of the proposed method.

To further verify the dual-layer optimization model proposed possesses better effects and performance, a detailed analysis is conducted from three aspects such as grid loss, voltage level, and DG allocation below. Based on the active power loss and node voltage level in the system, the results from Table A1 in Appendix A show that under nominal load

with five different scenarios ranging from 2 to 6, the active power grid loss in the system decreases sequentially as follows: 139.7431 kW, 92.2000 kW, 85.4004 kW, 67.9401 kW, and 65.4468 kW. The grid loss reduction rate gradually increases from 31.04% in scenario 2 to 67.70% in scenario 6. Additionally, the lowest node voltage magnitudes are recorded as 0.9378 p.u, 0.9738 p.u, 0.9599 p.u, 0.9747 p.u, and 0.9776 p.u. Clearly, the improvement effects are more pronounced in scenario 6, which demonstrates that the method proposed in this paper is more effective and practical compared with another four schemes.

From the perspective of the installed locations and capacities of the DGs, as shown in Table 1, under nominal load, scenarios 1 and 2 do not consider the DGs accessing the distributed grid. Therefore, our analysis primarily focuses on the optimization results from scenario 3 to scenario 6. Accordance to Table A1 in Appendix A, in scenario 3, the reactive node locations of the accessed DGs are 16, 18, and 31, with a total capacity of 2.0601 MW. In scenario 4, the aforementioned assess locations change into 18, 30, and 32, with a total capacity of 1.2120 MW. Scenario 5 yields the same results as scenario 3, while in scenario 6, the node positions of the accessed DGs change to 17, 30, and 31, with a total capacity of 2.1672 MW. From this perspective, scenario 6 has the highest accessed capacity for DGs, with a permeability rate of 58.34%. This high permeability rate indicates that DGs are effectively accessing the distribution network. Obviously, the proposed optimization method can effectively enhance the installed capacity of DGs accessing the distribution network. As a result, the locations where the DGs are installed become more reasonable and feasible compared to other scenarios.

In addition, from Table A1 in Appendix A, we can clearly see that the results obtained in scenario 3 are significantly better than those in scenario 2. The reason for this is that the assessed DGs directly contribute to offsetting a portion of the system loads, while distribution network reconfiguration only indirectly reduces the flow of system loads. When comparing scenario 3 with scenario 4, we observe that in scene 4, although the size of the accessed DGs is slightly higher than half of that in scenario 3, there are still lower grid loss and satisfactory voltage levels. This indicates that the role of distribution network reconfiguration should not be ignored. However, in scenario 5, the comprehensive indexes obtained are significantly better than those in scenario 4, even though both scenarios consider DG allocation and reconfiguration strategies. The reason for this difference lies in the implementation of different optimizing orders, leading to different desired aims. In practice, under the arrangement, the aim of the latter to be evolved is to expect to obtain one excellent topology to lessen the size of the DGs as soon as possible, and the one of the former is to obtain the optimal size of the DGs accessed under the current network topology. Clearly, at the moment, if we do not consider distribution network reconfiguration in scenario 5, the results should be the same as those in scenario 3. However, we also observe a significant drawback in scenario 5, which is that the optimized allocation of the DGs is only suitable for the current topology. Therefore, if the network topology changes, it may not always be suitable for the current network topology. However, this drawback is better addressed in scenario 6, resulting in more ideal results.

The analysis conducted on the optimization results, aiming at a load coefficient of 1.0 as mentioned above, reveals that this can be achieved by considering load coefficients of 0.5 and 1.6, respectively, as shown in Table A1 of Appendix A. From the analysis results, it is evident that the proposed dual-layer optimization model, namely scenario 6, exhibits better performance and provides a more effective scheme for distribution network reconfiguration, thereby improving the acceptable capacities of the DGs.

Figures 5–7 show the distribution of node voltage magnitude in the system under three different load levels. Each figure includes six scenarios for each load level.

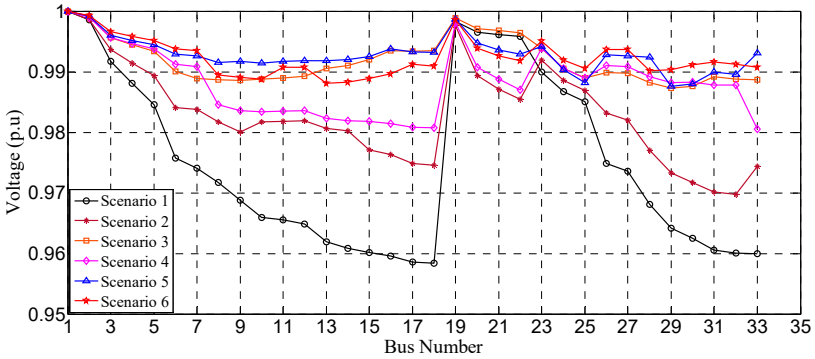


Figure 5. Voltage profile of 33-bus distribution at light load (0.5).

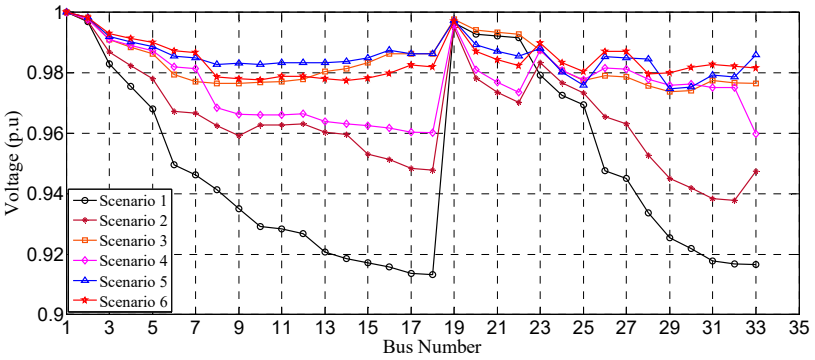


Figure 6. Voltage profile of 33-bus distribution at nominal load (1.0).

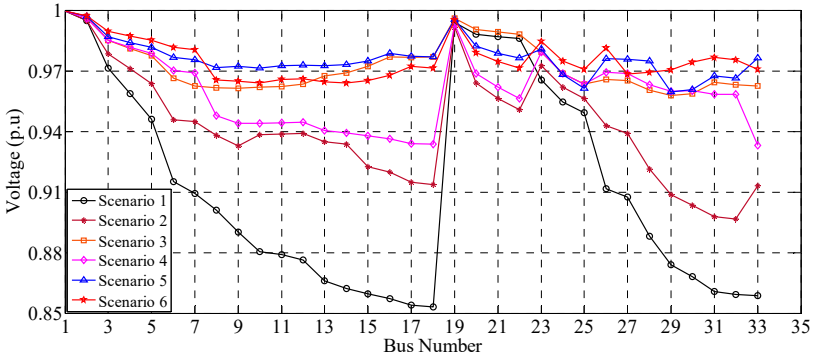


Figure 7. Voltage profile of 33-bus distribution at heavy load (1.6).

From Figures 5–7, it is evident that the node voltage deviation is larger in scenario 1 or 2. The main reason for this is that scenario 1 does not implement any optimization measures, while scenario 2 only considers reconfiguration. On the other hand, the node voltage deviation is relatively small in scenario 3, as it utilizes DG configuration to optimize the distribution network. However, in this situation, the system's permeability rate reaches 55.45%, indicating that the capacity of the accessed DGs is larger.

In scenarios 4 and 5, both distribution grid reconfiguration and DG configuration are considered in the optimization strategy. However, only in simple order, and the mutually dynamic connections are not fully balanced. In scenario 4, the permeability rate of the DGs is only 32.62%, which is a reduction of 22.83% compared to scenario 3. As a result, node-voltage deviation in scenario 4 is larger than in scenario 3. In scenario 5, the optimization allocation of DGs is considered first, without involving distribution grid reconfiguration. Then, more attention is given to distribution grid reconfiguration. This approach results in a permeability rate of 55.45%. Hence, the voltage enhancement effect in scenario 5 is better than in scenarios 3 and 4.

In scenario 6, the dual-layer optimization model proposed in this paper is applied, such that the voltage distribution of the system is more ideal and stable than the other five scenarios, the reasons lie in that it considers a mutually restrictive relationship between distribution grid reconfiguration and DGs optimization configuration. This demonstrates the effectiveness of the proposed optimization model in addressing the issue of larger node voltage deviation in the system.

In order to further illustrate the superiority of the dual-layer optimization model, a comparison of results is conducted with a load level coefficient of 1.0. This comparison is between the method proposed in this paper and two other methods achieved in [25,34]. The relevant results can be found in Table A2 of Appendix A. The studies conducted by Srinivasa [25] and Rajaram [30], respectively, applied the modified plant growth simulation algorithm (MPGSA) and the harmony search algorithm (HSA) to optimize the distribution networks. Five types of scenarios were selected for the optimization. It is important to note that in these investigations, scenario 5 only considers the locations and capacities of the DGs and the distribution grid reconfiguration. It does not reflect the mutually restrictive relationship between them.

From Table A2 in Appendix A, it can be observed that, except for scenario 1, the system demonstrates better performance in terms of grid loss, node voltage, and DG allocation under the remaining five scenarios when the method proposed in this paper is adopted. This indicates that the proposed model is a more scientific, reasonable, and effective method for distributed gird reconstruction that includes DGs.

Furthermore, in order to validate the effectiveness of the IHSA compared to the traditional HSA, both algorithms were applied to the IEEE 33 bus distribution system for comparative analysis. The parameter values for the IHSA remain the same as mentioned above, while the parameter values for the HSA are as follows: HMS = 50, HMCR = 0.90, PAR = 0.4, and Itr_{max} = 300. Finally, both algorithms were applied to scenario 6 with a load level coefficient of 1.0 to compare and analyze their optimization performance, as shown in Table 2 and Figure 8.

Table 2. Comparison of the results of 33 bus distribution network with different algorithms.

Algorithm	Reconfiguration Results	Active Power Loss (kW)	The Minimum Voltage (p.u)	Iteration Times
HSA	[7 13 10 32 28]	65.8501	0.9721	79
IHSA	[7 13 10 32 27]	65.4468	0.9776	63

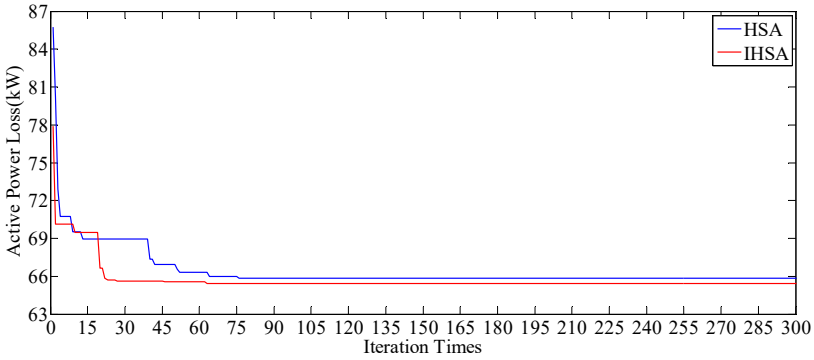


Figure 8. Convergence comparison of two algorithms in 33-bus distribution network.

As observed from Table 2 and Figure 8, it is evident that the IHSA exhibits significantly better convergence effects compared to the HSA, which can converge to the optimal solution with a smaller number of iterations at 63 times, whereas the HSA requires 79 times iteration before convergence, and the optimization result is not the optimal solution. Additionally, the HAS results in relatively high active power loss due to getting trapped in the

local optimum, preventing it from converging to the optimal solution. Hence, the IHSA demonstrates higher optimization efficiency and superior optimization performance.

5.2. 69-Bus Test System

To further showcase the versatility of the proposed bi-level optimization model, it is implemented on a larger scale radial distribution system (69-bus system). This system comprises 69 nodes and 73 branches. Similar to the 33-bus system, the system consists of 68 section switches (1–68) and 5 tie switches (69–73), as depicted in Figure 9. The system operates at a voltage of 12.66 kV and has a total load of 3802.19 + j2694.60kVA. The system parameters and load data can be found in ref. [35].

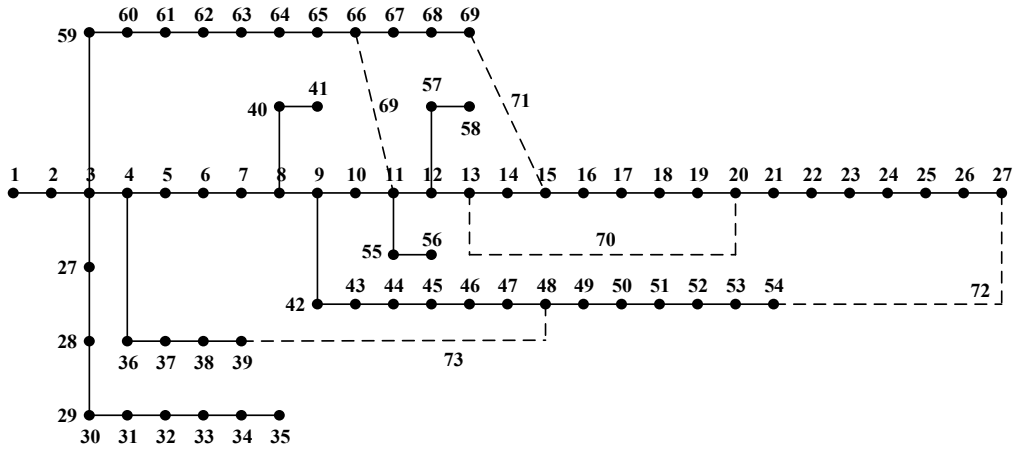


Figure 9. PG&E 69-bus distribution system.

Similar to the 33-bus system, the test system in question is also optimized under six different scenarios and three distinct load levels. The optimization results can be found in Table A3 of Appendix A. Through an analysis of the three key aspects of grid loss, voltage level, and acceptable capacities of the DGs, it is evident that scenario 6 possesses better performance in reducing power loss and increasing the size of DGs compared to the other five scenarios. Additionally, the node-voltage distribution in scenario 6 is more ideal and stable compared to the other five scenarios, as illustrated in Figures 10–12.

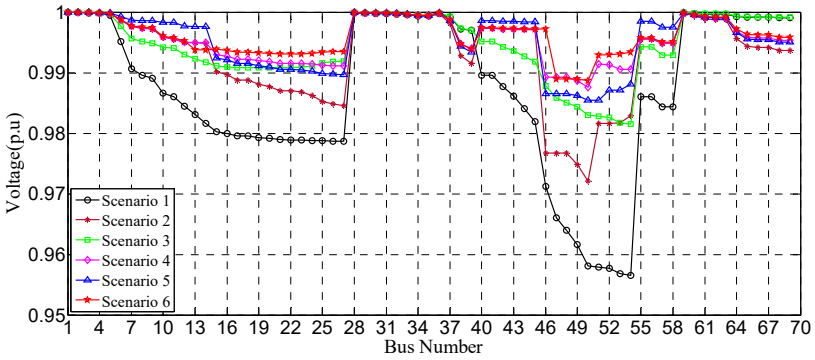


Figure 10. Voltage profile of 69-bus distribution at light load (0.5).

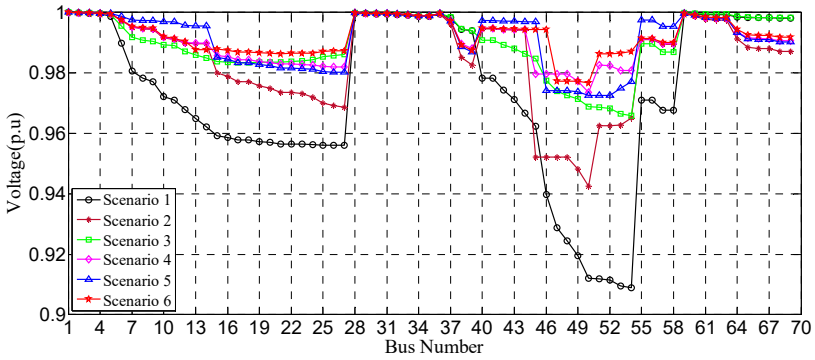


Figure 11. Voltage profile of 69-bus distribution at nominal load (1.0).

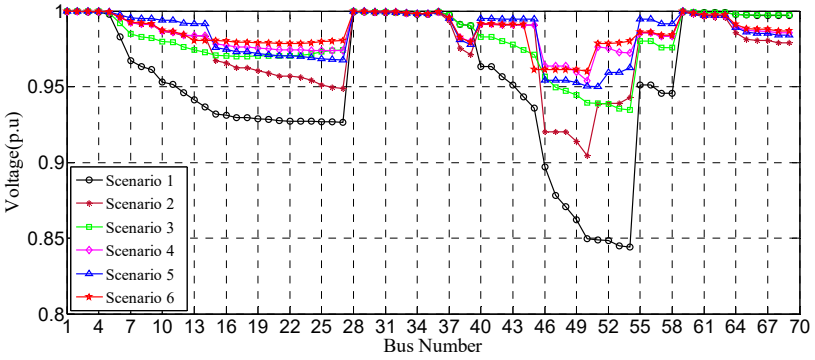


Figure 12. Voltage profile of 69-bus distribution at heavy load (1.6).

In addition, to further demonstrate the superiority of the proposed bi-level optimization model for distribution network reconfiguration in enhancing the acceptable capacities of the DGs, the results are compared with the [25] as shown in Table A4 of Appendix A. It is evident from the table that the proposed bi-level optimization model is better than the ones of GA and RGA in terms of solution quality across all scenarios. Meanwhile, it can be seen from Table 3 and Figure 13 that the convergence effect of IHSA that applied to the 69-bus system also can be obviously better than that of HAS.

Table 3. Comparison of the results of 69-node reconstruction with different algorithms.

Algorithm	Reconfiguration Results	Active Power Loss (kW)	The Minimum Voltage (p.u)	Iteration Times
HSA	[69 70 12 50 47]	39.4354	0.9747	131
IHSA	[69 70 12 50 44]	39.2642	0.9768	117

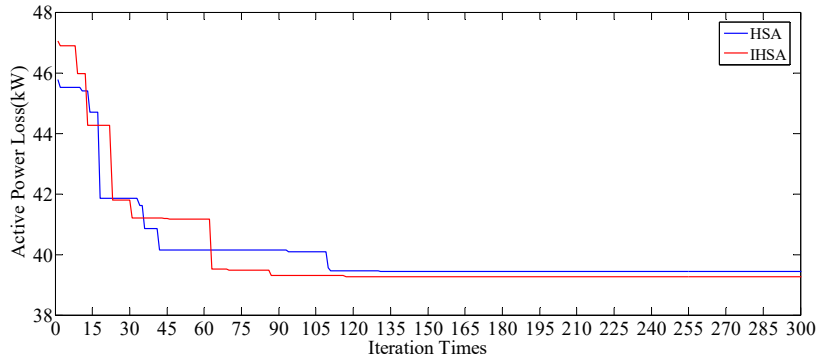


Figure 13. Convergence comparison of two algorithms in 69-bus distribution network.

Based on the two aforementioned examples, it is evident that the bi-level optimization model proposed in this paper is applicable to both small-scale distribution networks and large-scale distribution networks. In particular, it is more dramatic for the numerous large-size heavy-load distributed networks in China to realize energy saving and emission reduction. At the same time, it can show better performance and achieve better results in all aspects. This shows that the proposed dual-layer optimization model is feasible and scientific, and could be used to solve the complicated DG allocation issue in distributed networks, especially under smart environments.

6. Conclusions

This paper proposes a bi-level optimization model that simultaneously addresses the distributed network topology and grid-connected capacity of DG under the VPP and smart grid. The model fully considers the interactive correlation between them, allowing for cyclic iterative optimization to obtain the optimal solution that includes both the network topology and the maximum grid-connected capacities of DGs. It should be pointed out that the optimized results obtained from this model are indeed superior to those of traditional methods. This is because the model considers a larger solution space, which possibly leads to inadaptability in applications. However, with the advancements in VPP and smart grid technologies, these concerns will gradually be dispelled. In addition, the two-level optimization model presented in this paper is highly inclusive, which can also be applied as a traditional model, i.e., a single-layer optimization model, by keeping one of the upper or lower models unchanged during optimization, whereas the results obtained by bi-layer optimization can be used as the desired values to evaluate them, and so it possesses significant theoretical reference value. From an algorithmic perspective, this paper divides the entire problem-solving space into two stages based on different desired goals. This approach is similar to the back/forward sweep method used in the power flow algorithm for radial power networks under the known initial end voltage and terminal power. By doing so, the convergence and effectiveness of the algorithm can be significantly enhanced. Moreover, the presented bi-level optimization model may be much easier to apply by implementing some limitations on upper and lower-layer aim functions or changing them since it tightens solution space by releasing some free variables, this is quite important to facilitate large-scale applications of DERs from reality technique basis and application preference. The proposed bi-level optimization model fully harnesses the potential of a distributed network to achieve maximum energy conservation and emission reduction. It also serves as a valuable theoretical and technical reference for other similar optimization problems. In this paper, we have conducted extensive research on the optimal scheduling of DGs and have obtained significant research outcomes. Nevertheless, there exist certain constraints. The bi-level optimization model proposed for scheduling is a result of research conducted under ideal conditions. When simultaneous scheduling of both upper and lower layers is performed, this model enhances the optimization of distribution network topology, alongside the determination of DGs' location and capacity. This, however, results in significant computational demands, posing challenges for practical implementation. Moreover, the algorithm produces refined optimization results, serving as a valuable benchmark for assessing the performance of alternative algorithms. In the upcoming phase of our research, we will explore the feasibility of implementing this algorithm in real-world engineering applications.

Author Contributions: Conceptualization, H.S. and X.W.; methodology, H.S. and X.W.; software, X.W. and Z.D.; validation, X.W.; formal analysis, X.W. and H.S.; investigation, X.W. and H.S.; resources, Z.D.; data curation, H.S. and Z.D.; writing—original draft preparation, X.W.; writing—review and editing, X.W. and H.S.; visualization, X.W. and Z.D.; supervision, H.S.; project administration, H.S.; funding acquisition, H.S. All authors have read and agreed to the published version of the manuscript.

Funding: This research was funded by the National Nature Science Foundation of China, grant number 61867003, and the Key Project of Science and Technology Research and Development Plan of China Railway Co., Ltd. (Lanzhou, China), grant number N2022X009.

Data Availability Statement: The data used to support the findings of the study are included in this paper.

Acknowledgments: The authors would like to express our sincere appreciation to the anonymous referees for providing valuable suggestions and comments that have significantly contributed to the improvement of our manuscript.

Conflicts of Interest: The authors declare no conflict of interest.

Appendix A

Table A1. Simulation results of 33-bus system.

Scenario	Item	Load Level		
		Light (0.5)	**Nominal (1.0)**	**Heavy (1.6)**
Base Case (Scenario 1)	Switches Opened	33, 34, 35, 36, 37	33, 34, 35, 36, 37	33, 34, 35, 36, 37
	Power Loss (kW)	47.0644	202.6471	575.2623
	Minimum Voltage (p.u)	0.9584	0.9133	0.8532
Only Reconfiguration (Scenario 2)	Switches Opened	7, 14, 9, 32, 37	7, 14, 9, 32, 37	7, 14, 9, 32, 37
	Power Loss (kW)	33.2513	139.7431	380.2175
	Minimum Voltage (p.u)	0.9698	0.9378	0.8967
	Loss Reduction (%)	29.35	31.04	33.91
Only DG Installation (Scenario 3)	Switches Opened	33, 34, 35, 36, 37	33, 34, 35, 36, 37	33, 34, 35, 36, 37
	Size of DG (MW) (Candidate Bus)	0.3375 [bus 16] 0.1079 [bus 18] 0.5826 [bus 31]	0.6781 [bus 16] 0.2170 [bus 18] 1.1650 [bus 31]	1.0850 [bus 16] 0.3440 [bus 18] 1.9286 [bus 31]
	Power Loss (kW)	22.2786	92.2000	247.5140
	Minimum Voltage (p.u)	0.9873	0.9738	0.9580
	Loss Reduction (%)	52.66	54.50	56.97
DG Installation after Reconfiguration (Scenario 4)	Switches Opened	7, 14, 9, 32, 37	7, 14, 9, 32, 37	7, 14, 9, 32, 37
	Size of DG (MW) (Candidate Bus)	0.0936 [bus 18] 0.3380 [bus 30] 0.1756 [bus 32]	0.1798 [bus 18] 0.6786 [bus 30] 0.3536 [bus 32]	0.2725 [bus 18] 1.0837 [bus 30] 0.5526 [bus 32]
	Power Loss (kW)	20.6288	85.4004	228.6926
	Minimum Voltage (p.u)	0.9805	0.9599	0.9333
	Loss Reduction (%)	56.17	57.86	60.25
Reconfiguration after DG Installation (Scenario 5)	Switches Opened	7, 12, 10, 32, 28	7, 12, 10, 32, 28	7, 12, 10, 32, 28
	Size of DG (MW) (Candidate Bus)	0.3375 [bus 16] 0.1079 [bus 18] 0.5826 [bus 31]	0.6781 [bus 16] 0.2170 [bus 18] 1.1650 [bus 31]	1.0850 [bus 16] 0.3440 [bus 18] 1.9286 [bus 31]
	Power Loss (kW)	16.5002	67.9401	180.4301
	Minimum Voltage (p.u)	0.9876	0.9747	0.9597
	Loss Reduction (%)	64.94	66.47	68.64

Table A1. *Cont.*

Scenario	Item	Load Level		
		Light (0.5)	**Nominal (1.0)**	**Heavy (1.6)**
Bi-level Optimization Model (Scenario 6)	Switches Opened	7, 12, 10, 32, 27	7, 13, 10, 32, 27	7, 13, 10, 32, 26
	Size of DG (MW) (Candidate Bus)	0.3619 [bus 17] 0.4125 [bus 30] 0.3314 [bus 31]	0.6825 [bus 17] 0.7927 [bus 30] 0.6920 [bus 31]	1.1112 [bus 17] 1.4301 [bus 30] 1.2312 [bus 31]
	Power Loss (kW)	15.9349	65.4468	177.6714
	Minimum Voltage (p.u)	0.9881	0.9776	0.9642
	Loss Reduction (%)	66.14	67.70	69.11

Table A2. Comparison of simulation results of 33-bus system.

Scenario	Item	Method Comparison		
		The Proposed Method	**MPGSA (30)**	**HAS (21)**
Base Case (Scenario 1)	Switches Opened	33, 34, 35, 36, 37	33, 34, 35, 36, 37	33, 34, 35, 36, 37
	Power Loss (kW)	202.6471	202.67	202.67
	Minimum Voltage (p.u)	0.9133	0.9052	0.9131
Only Reconfiguration (Scenario 2)	Switches Opened	7, 14, 9, 32, 37	7, 14, 9, 32, 37	7, 14, 9, 32, 37
	Power Loss (kW)	139.7431	139.5	138.06
	Minimum Voltage (p.u)	0.9378	0.9343	0.9342
	Loss Reduction (%)	31.04	31.17	31.88
Only DG Installation (Scenario 3)	Switches Opened	33, 34, 35, 36, 37	33, 34, 35, 36, 37	33, 34, 35, 36, 37
	Size of DG (MW) (Candidate Bus)	0.6781 [bus 16] 0.2170 [bus 18] 1.1650 [bus 31]	0.1058 [bus 17] 0.5900 [bus 18] 1.0812 [bus 31]	0.5724 [bus 17] 0.1070 [bus 18] 1.0462 [bus 33]
	Power Loss (kW)	92.2000	95.42	96.76
	Minimum Voltage (p.u)	0.9738	0.9585	0.9670
	Loss Reduction (%)	54.50	52.92	52.26
DG Installation after Reconfiguration (Scenario 4)	Switches Opened	7, 14, 9, 32, 37	7, 9, 13, 32, 37	7, 14, 9, 32, 37
	Size of DG (MW) (Candidate Bus)	0.1798 [bus 18] 0.6786 [bus 30] 0.3536 [bus 32]	0.2469 [bus 30] 0.1795 [bus 31] 0.6645 [bus 32]	0.6612 [bus 30] 0.1611 [bus 31] 0.2686 [bus 32]
	Power Loss (kW)	85.4004	92.87	97.13
	Minimum Voltage (p.u)	0.9599	0.9482	0.9479
	Loss Reduction (%)	57.86	54.18	52.07

Table A2. *Cont.*

Scenario	Item	Method Comparison		
		The Proposed Method	**MPGSA (30)**	**HAS (21)**
Reconfiguration after DG Installation (Scenario 5)	Switches Opened	7, 12, 10, 32, 28	-	-
	Size of DG (MW) (Candidate Bus)	0.6781 [bus 16] 0.2170 [bus 18] 1.1650 [bus 31]	- - -	- - -
	Power Loss (kW)	67.9401	-	-
	Minimum Voltage (p.u)	0.9747	-	-
	Loss Reduction (%)	66.47	-	-
Scenario 6	Switches Opened	7, 13, 10, 32, 27	7, 14, 10, 28, 31	7, 14, 10, 28, 32
	Size of DG (MW) (Candidate Bus)	0.6825 [bus 17] 0.7927 [bus 30] 0.6920 [bus 31]	0.6311 [bus 18] 0.5568 [bus 32] 0.5986 [bus 33]	0.5586 [bus 31] 0.5258 [bus 32] 0.5840 [bus 33]
	Power Loss (kW)	65.4468	72.23	73.05
	Minimum Voltage (p.u)	0.9776	0.9724	0.9700
	Loss Reduction (%)	67.70	64.36	63.59

Table A3. Simulation results of 69-bus system.

Scenario	Item	Load Level		
		Light (0.5)	**Nominal (1.0)**	**Heavy (1.6)**
Base Case (Scenario 1)	Switches Opened	69, 70, 71, 72, 73	69, 70, 71, 72, 73	69, 70, 71, 72, 73
	Power Loss (kW)	51.9403	226.4735	656.9548
	Minimum Voltage (p.u)	0.9566	0.9089	0.8440
Only Reconfiguration (Scenario 2)	Switches Opened	69, 70, 14, 50, 45	69, 70, 14, 50, 44	69, 70, 14, 50, 45
	Power Loss (kW)	24.0431	100.9662	275.8305
	Minimum Voltage (p.u)	0.9721	0.9425	0.9044
	Loss Reduction (%)	53.71	55.42	58.01
Only DG Installation (Scenario 3)	Switches Opened	69, 70, 71, 72, 73	69, 70, 71, 72, 73	69, 70, 71, 72, 73
	Size of DG (MW) (Candidate Bus)	0.1156 [bus 27] 0.6398 [bus 50] 0.2180 [bus 55]	0.2606 [bus 27] 1.3796 [bus 50] 0.4686 [bus 55]	0.4155 [bus 27] 1.9835 [bus 50] 0.6520 [bus 55]
	Power Loss (kW)	19.4053	76.4004	218.4006
	Minimum Voltage (p.u)	0.9815	0.9659	0.9346
	Loss Reduction (%)	62.64	66.27	66.76

Table A3. *Cont.*

Scenario	Item	Load Level		
		Light (0.5)	**Nominal (1.0)**	**Heavy (1.6)**
DG Installation after Reconfiguration (Scenario 4)	Switches Opened	69, 70, 14, 50, 45	69, 70, 14, 50, 44	69, 70, 14, 50, 45
	Size of DG (MW) (Candidate Bus)	0.2560 [bus 48] 0.5260 [bus 50] 0.1809 [bus 51]	1.1316 [bus 48] 0.5424 [bus 50] 0.3610 [bus 51]	1.5148 [bus 48] 0.9589 [bus 50] 0.6570 [bus 51]
	Power Loss (kW)	10.0542	44.1955	113.2081
	Minimum Voltage (p.u)	0.9876	0.9736	0.9540
	Loss Reduction (%)	80.64	80.49	82.77
Reconfiguration after DG Installation (Scenario 5)	Switches Opened	69, 70, 14, 51, 45	69, 70, 14, 52, 45	69, 70, 14, 51, 45
	Size of DG (MW) (Candidate Bus)	0.1156 [bus 27] 0.6398 [bus 50] 0.2180 [bus 55]	0.2606 [bus 27] 1.3796 [bus 50] 0.4686 [bus 55]	0.4155 [bus 27] 1.9835 [bus 50] 0.6520 [bus 55]
	Power Loss (kW)	9.9789	39.6613	107.9193
	Minimum Voltage (p.u)	0.9854	0.9726	0.9502
	Loss Reduction (%)	80.79	82.49	83.57
Bi-level Optimization Model (Scenario 6)	Switches Opened	69, 70, 12, 50, 46	69, 70, 12, 50, 46	69, 70, 12, 50, 44
	Size of DG (MW) (Candidate Bus)	0.7650 [bus 50] 0.1296 [bus 53] 0.1236 [bus 54]	1.5193 [bus 50] 0.2536 [bus 53] 0.2680 [bus 54]	2.3369 [bus 50] 0.3551 [bus 53] 0.5054 [bus 54]
	Power Loss (kW)	9.6358	39.2642	102.8482
	Minimum Voltage (p.u)	0.9887	0.9768	0.9600
	Loss Reduction (%)	81.45	82.66	84.34

Table A4. Comparison of simulation results of 69-bus system.

Scenario	Item	Method Comparison		
		Proposed Method	**GA**	**RGA**
Scenario 2	Switches Opened	69, 70, 14, 50, 44	69, 18, 13, 56, 61	69, 17, 13, 55, 61
	Power Loss (kW)	100.9662	99.35	100.28
	Minimum Voltage (p.u)	0.9425	0.9428	0.9428
	Loss Reduction (%)	55.42	55.85	55.42
Scenario 3	Switches Opened	69, 70, 71, 72, 73	69, 70, 71, 72, 73	69, 70, 71, 72, 73
	Size of DG (MW)	2.1088	1.7732	1.7868
	Power Loss (kW)	76.4004	86.77	87.65
	Minimum Voltage (p.u)	0.9659	0.9677	0.9678
	Loss Reduction (%)	66.27	61.43	61.04
Scenario 4	Switches Opened	69, 70, 14, 50, 44	69, 18, 13, 56, 61	69, 17, 13, 55, 61
	Size of DG (MW)	2.0350	1.8448	1.6396
	Power Loss (kW)	44.1955	51.30	52.34
	Minimum Voltage (p.u)	0.9736	0.9619	0.9611
	Loss Reduction (%)	80.49	77.20	76.73
Scenario 6	Switches Opened	69, 70, 12, 50, 46	69, 17, 13, 58, 61	10, 16, 14, 55, 62
	Size of DG (MW)	2.0409	1.8718	2.0654
	Power Loss (kW)	39.2642	40.30	44.23
	Minimum Voltage (p.u)	0.9768	0.9736	0.9742
	Loss Reduction (%)	82.66	82.08	80.32

References

1. Jenkins, N.; Ekanayake, J.B.; Strbac, G. *Distributed Generation*; The Institution of Engineering and Technology: London, UK, 2010.
2. Su, H. Sitting and Sizing of Distributed Generation Based on Improved Simulated Annealing Particle Swarm Optimization. *Environ. Sci. Pollut. Res.* **2019**, *26*, 17927–17938. [CrossRef] [PubMed]
3. Awerbuch, S.; Preston, A. *The Virtual Utility: Accounting, Technology & Competitive Aspects of the Emerging Industry*; Springer: Berlin/Heidelberg, Germany, 1997.
4. Chen, C.; Li, N.; Zhong, P.; Zeng, M. Review of virtual power plant technology abroad and enlightenment to China. *Power Syst. Technol.* **2009**, *37*, 2258–2263.
5. Yu, J.; Zhang, F. Distribution network reconfiguration based on improved immune genetic algorithm. *Power Syst. Technol.* **2009**, *33*, 100–105.
6. Wang, J.; Lv, L.; Liu JHu, C.; Zhu, Y. Reconfiguration of distribution network containing distribution generation units based on improved layered forward-backward sweep method. *Power Syst. Technol.* **2010**, *34*, 60–64. [CrossRef]
7. He, Y.; Peng, J.W.; Mao, L. Scenario model and algorithm for the reconfiguration of distribution network with wind power generators. *Proc. CSEE* **2010**, *30*, 12–18.
8. Tian, H.; Lv, L.; Gao, H.; Li, M.; Wang, G.; Cheng, S.; Zhu, X. Dynamic reconfiguration of distribution network considering power grid operation characteristic. *Power Syst. Prot. Control* **2015**, *43*, 9–14.
9. Behdad, A.; Hooshmand, R.; Gholipour, E. Decreasing activity cost of a distribution system company by reconfiguration and power generation control of DGs based on shuffled frog leaping algorithm. *Electr. Power Syst. Res.* **2014**, *61*, 48–55.
10. Chen, D.; Zhang, X. Distribution network reconfiguration of distributed generation based on amopso algorithm. *Acta Energ. Solaris Sin.* **2017**, *38*, 2195–2203.
11. Li, Z.; Chen, X.; Yu, K.; Liu, H.; Zhao, B. Hybrid particle swarm optimization for distribution network reconfiguration. *Proc. CSEE* **2008**, *28*, 35–41.
12. Xiang, X.; Liao, D.; Xiang, N.; Wang, B. Distribution network reconfiguration based on parallel Tabu search algorithm. *Power Syst. Technol.* **2012**, *36*, 100–105.
13. Xue, Y.; Wu, X.; Wei, W. Distribution network reconfiguration with BPSO based on combination of loop group search and individual loop replacement. *Power Syst. Technol.* **2016**, *40*, 263–269.
14. Ji, X.; Liu, Q.; Yu, Y. Two-level reconfiguration algorithm based on power moment and neighbourhood searching for distribution network. *Electr. Power Autom. Equip.* **2017**, *37*, 28–34.
15. Nasiraghdam, H.; Jadid, S. Optimal hybrid PV/WT/FC sizing and distribution system reconfiguration using multi-objective artificial bee colony (MOABC) algorithm. *Sol. Energy* **2012**, *86*, 3057–3071. [CrossRef]
16. Rosseti, G.; de Oliveira, E.; de Oliveira, L.; Silva, J.; Peres, W. Optimal allocation of distributed generation with reconfiguration in electric distribution systems. *Electr. Power Syst. Res.* **2013**, *103*, 178–183. [CrossRef]
17. Mohamed, I.A.; Kowsalya, M.; Kothari, D. A novel integration technique for optimal network reconfiguration and distributed generation placement in power distribution networks. *Elect. Power Energy Syst.* **2014**, *63*, 461–472. [CrossRef]
18. Bayat, A.; Bagheri, A.; Noroozian, R. Optimal siting and sizing of distributed generation accompanied by reconfiguration of distribution networks for maximum loss reduction by using a new UVDA-based heuristic method. *Int. J. Electr. Power Energy Syst.* **2016**, *77*, 360–371. [CrossRef]
19. Yin, X.; Ye, C.; Ding, Y.; Song, Y. Exploiting Internet Data Centers as Energy Prosumers in Integrated Electricity-Heat System. *IEEE Trans. Smart Grid* **2023**, *14*, 167–182. [CrossRef]
20. Xu, Y.; Liu, Z.; Zhang, C.; Ren, J.; Zhang, Y.; Shen, X. Blockchain-Based Trustworthy Energy Dispatching Approach for High Renewable Energy Penetrated Power Systems. *IEEE Internet Things J.* **2022**, *9*, 10036–10047. [CrossRef]
21. Mansouri, S.A.; Ahmarinejad, A.; Nematbakhsh, E.; Javadi, M.S.; Nezhad, A.E.; Catalao, J.P.S. A Sustainable Framework for Multi-Microgrids Energy Management in Automated Distribution Network by Considering Smart Homes and High Penetration of Renewable Energy Resources. *Energy* **2022**, *245*, 123228. [CrossRef]
22. Li, Y.; Gao, D.W.; Gao, W.; Zhang, H.; Zhou, J. A Distributed Double-Newton Descent Algorithm for Cooperative Energy Management of Multiple Energy Bodies in Energy Internet. *IEEE Trans. Ind. Inform.* **2021**, *17*, 5993–6003. [CrossRef]
23. Ameli, A.; Shahab, B.; Farid, K.; Mahmood, R.H. A multiobjective particle swarm optimization for sizing and placement of DGs from DG Owner's and distribution company's viewpoints. *IEEE Trans. Power Deliv.* **2014**, *9*, 1831–1840. [CrossRef]
24. Su, H.; Zhang, Z. Power Flow algorithm for weakly meshed distribution network with distributed generation based on loop-analysis in different load models. *J. Electr. Eng. Technol.* **2018**, *13*, 608–619.
25. Srinivasa, R.; Ravindra, K.; Satisk, K.; Narasimham, S. Power loss minimization in distribution system using network reconfiguration in the presence of distributed generation. *IEEE Trans. Power Syst.* **2013**, *28*, 317–325.
26. Wang, X.; Wei, Z.; Sun, G.; Li, Y.; Zang, H. Multi-objective distribution network reconfiguration considering uncertainties of distributed generation and load. *Electr. Power Autom. Equip.* **2016**, *36*, 116–121.
27. Chen, C.; Wang, F.; Liu, B.; Cao, Y.; Huang, C.; Dong, X. Network reconfiguration based on basic ring matrix and improved harmony search algorithm. *Autom. Electr. Power Syst.* **2014**, *38*, 55–60.
28. Geem, Z.; Kim, J.; Loganathan, G. A new heuristic optimization algorithm: Harmony search. *Simulation* **2001**, *76*, 60–68. [CrossRef]
29. Li, Z. An Adaptive Harmony Search Algorithm for Network Reconfiguration Considering Reliability. Master's Thesis, Zhejiang University, Hangzhou, China, 2017.

30. Jiang, Y.; Chen, Z.; Huang, C.; Cao, Y.; Sun, Y.; Jia, T. Distribution network reconfiguration based on heuristic rules and harmony search algorithm. *J. Hunan Univ. Nat. Sci. Ed.* **2014**, *4*, 61–67.
31. Liang, S. Distribution Network Reconfiguration Based on Improved Harmony Search Algorithm. Master's Thesis, Hunan University, Changsha, China, 2016.
32. Mistry, K.; Roy, R. Enhancement of loading capacity of distribution system through distributed generator placement considering technoeconomic benefits with load growth. *Int. J. Electr. Power Energy Syst.* **2014**, *54*, 505–515. [CrossRef]
33. Baran, M.; Wu, F. Network reconfiguration in distribution systems for loss reduction and load balancing. *IEEE Trans. Power Deliv.* **1989**, *4*, 1401–1409. [CrossRef]
34. Rajaram, R.; Kumar, S.; Rajasekar, N. Power system reconfiguration in a radial distribution network for reducing losses and to improve voltage profile using modified plant growth simulation algorithm with Distributed Generation (DG). *Energy Rep.* **2015**, *1*, 116–122. [CrossRef]
35. Savier, J.S.; Das, D. Impact of Network Reconfiguration on Loss Allocation of Radial Distribution Systems. *IEEE Trans. Power Deliv.* **2007**, *22*, 2473–2480. [CrossRef]

Disclaimer/Publisher's Note: The statements, opinions and data contained in all publications are solely those of the individual author(s) and contributor(s) and not of MDPI and/or the editor(s). MDPI and/or the editor(s) disclaim responsibility for any injury to people or property resulting from any ideas, methods, instructions or products referred to in the content.